Available online at www.sciencedirect.com
ScienceDirect
European Journal of Medicinal Chemistry 41 (2006) 1253–1261
EUROPEAN JOURNAL OF MEDICINAL CHEMISTRY
http://france.elsevier.com/direct/ejmech

Original article

Synthesis and characterization of novel hydrazide–hydrazones and the study of their structure–antituberculosis activity

Koçyiğit-Kaymakçıoğlu Bedia[a], Oruç Elçin[a], Unsalan Seda[a], Kandemirli Fatma[b], Shvets Nathaly[c], Rollas Sevim[a,*], Anatholy Dimoglo[c,d,*]

[a] *Department of Pharmaceutical Chemistry, Faculty of Pharmacy, Marmara University, Haydarpaşa 34668, Istanbul, Turkey*
[b] *Department of Chemistry, Kocaeli University, Umuttepe, 41380, Kocaeli, Turkey*
[c] *Gebze Institute of Technology, Cayirova, Gebze 41400, Kocaeli, Turkey*
[d] *Institute of Applied Physics, Academy of Sciences, MD2028 Kishinev, Moldova*

Received 1 February 2006; received in revised form 31 March 2006; accepted 15 June 2006
Available online 17 August 2006

Abstract

A series of hydrazide–hydrazones, based on a series of 4-substituted benzoic acid, were synthesized, and their structures were elucidated and screened for the antituberculosis activity against *Mycobacterium tuberculosis* H37Rv with the help of the BACTEC 460 radiometric system. Compound **3**, 4-fluorobenzoic acid [((5-nitro)thiophen-2yl) methylene]hydrazide showed the highest inhibitory activity in this series. The search of pharmacophores was done by means of the Electronic-Topological Method (ETM). The model developed in this study is supposed to be applied to the design, preparation and screening of new compounds of similar structure in order to further test and optimize the model with the eventual goal of preparing new anti-tubercular agents.

Keywords: Antituberculosis activity; Hydrazide–hydrazones; Structure–activity relationships

1. Introduction

Tuberculosis is presently regarded as the most dangerous infective disease world-wide and one of the major AIDS-associated infections. The simultaneous presence of HIV infection, the spread of drug resistant strains of *Mycobacterium tuberculosis*, and the scarce compliance with the lengthy complex therapies often complicate the treatment of tuberculosis [1]. Therefore, the search for new antituberculosis agents is required. This requirement had an impact on our further work on the synthesis and search for some new hydrazide–hydrazones with the antituberculosis activity.

It is well known that the hydrazone group plays an important role for the antimicrobial activity. Furthermore, a number of hydrazide–hydrazone derivatives have been claimed to possess interesting antibacterial–antifungal [2–4], anticonvulsant [5–7], antiinflammatory [8,9], antimalarial [10] and antituberculosis activities [11–17]. We described previously the antimicrobial profile of hydrazide–hydrazone derivatives of 4-fluorobenzoic acide, some of which have exhibited a remarkable antimicrobial activity [18]. With the aim of obtaining new antimycobacterial compounds we synthesized a series of 4-substituted benzoic acid (substituted methylene) (**3**–**31**) hydrazide derivatives in which the nitrophenyl/furanyl moiety of the previously described compounds was replaced by the substituted phenyl, furanyl, pyrolyl or thiophenyl moiety.

The named compounds were evaluated for the antimycobacterial activity; on account of biological profile of some previously synthesized hydrazide–hydrazones [18], the new hydrazide–hydrazone derivatives were tested in vitro as to their activities against *M. tuberculosis* H37Rv.

The present study used the Electronic-Topological Method (ETM) to build the system capable of predicting antituberculosis activities. The ETM is a structure-based approach for studying structure–activity relationships (SAR) of molecules [19]. As known, more informative molecular descriptions in terms

* Corresponding authors.
E-mail addresses: sevim@sevimrollas.com (K.-K. Bedia), dimoglo@gyte.edu.tr (A. Dimoglo).

0223-5234/$ - see front matter © 2006 Elsevier Masson SAS. All rights reserved.
doi:10.1016/j.ejmech.2006.06.009

of their structural and electron parameters cause better results in pattern recognition and separation of molecules by the activity levels. ETM is capable of taking into account individual properties of separate atoms and bonds that may be crucial for revealing details of interactions between a biologic receptor and an active molecule. A number of studies have been reported that use the ETM to find SAR models involving a representative list of activities and thousands of compounds belonging to different chemical classes [20–23]. The ETM approach and software have both undergone considerable development [24–26]. The new ETM-based system capable of unifying Web-based SAR resources and using Internet communications in the framework of a project, ETOSAR, makes the ETM a valuable tool for SAR studies and provides rules for the synthesis of new potentially active compounds [27–29].

2. Chemistry and biological activity testing

The synthesis of starting compounds, 4-substituted benzoic acid hydrazide derivatives **2a**–**d** was carried out by treating 4-substituted phenyl benzoate **1a**–**d** with hydrazine hydrate (see [30] for the procedure), while 4-nitrobenzoic acid hydrazide **2e** was prepared by the reaction of 4-nitrobenzoyl chloride with hydrazine hydrate. The hydrazones **3**–**31** (Table 1) were prepared through the synthetic pathway shown in Scheme 1, from the reaction of equimolar amounts of properly 4-substituted benzoic acid hydrazide with substituted aldehydes in the presence of ethanol.

Physicochemical and spectroscopic characterization of the hydrazones **6**, **7** [17], **8**, **10**, **15** [18], **13**, **30** [31] and **29** [32] as well as of compounds **21**, **31** [33] have been previously described. The other newly described here hydrazone compounds were isolated in satisfactory yields (40–97%) and purified (recrystallized with the use of ethanol). Their chemical structures were confirmed by ^{1}H-NMR, mass (MS-ES), and elemental analysis. The hydrazone –CH= and –NH– signal of novel synthesized compounds appeared as a singlet at 8.16–8.67 and 10.45–12.25 ppm, respectively. The signal of aromatic protons was also found in the expected field.

The in vitro antimycobacterial evaluation was performed according to the TAACF antituberculosis drug discovery program [34]. The primary screening data for all compounds were shown in Table 1. The results of the study on the antituberculosis activity showed that compound **3** exhibited highest inhibition (99%) at a constant concentration level (6.25 μg/ml) against *M. tuberculosis* H37Rv. Compounds **3**–**7** effecting ≥ 90% inhibition in the primary screen at 6.25 μg/ml were re-tested at lower concentration against *M. tuberculosis* H37Rv using microplate alamar blue assay (MABA) to determine the actual minimum inhibitory concentration (MIC) in a broth microdilution assay. The MIC is defined as the lowest concentration effecting the 90% reduction in fluorescence, relative to controls. Compound **5** demonstrated potent inhibitory activity against *M. tuberculosis* H37Rv by a MIC value of 0.78 μg/ml. Compound **3**, **6** and **7** demonstrated same inhibitory activity by a MIC value of 3.13 μg/ml, whereas compound **4**, which was selected for the level 2 screening, did not possess a MIC less than 6.25 μg/ml. In addition, IC_{50} and selectivity index value (SI) were determined 1.28, 0.41 for compound **3**; 0.48, 0.62 μg/ml for compound **5**; 0.41, 0.13 for compound **6**, respectively.

3. Results and discussion

3.1. The search for pharmacophores (Ph) and anti-pharmacophores (APh) by using ETM

The compounds under study (29 molecules) are shown in Table 1. Molecules were classified as either active or inactive ones. Conformational analysis and quantum chemistry calculations were carried out by means of the molecular mechanics method (MMP2) and the semi-empirical quantum chemistry method (AM1), respectively [35]. All obtained data were arranged as matrices called electronic-topological matrices of contiguity (ETMC). Diagonal elements of the matrices reflect one or more possible atomic properties (represented by a separate value or by a vector of characteristics). Off-diagonal elements characterize bonds between pairs of atoms, if they exist, or distances otherwise. The matrices are symmetric relative to their diagonals that is why only their upper triangles are used in calculations. For the sake of simplification, the ETM calculations generally use only by one property for atoms and bonds. In cases when more than by one property for atoms and bonds is needed, the ETM calculations can be repeated separately for each pair of atom–bond properties. In our case, effective charges on atoms are taken as diagonal elements, and the values of Wiberg's index represent off-diagonal elements corresponding to bonds; if no bond, then off-diagonal elements are distances for corresponding pairs of atoms in 3D-space.

The computational part of the ETM is a sequence of the following steps [36–38]:

- conformational analysis;
- quantum-chemistry calculations;
- ETMC formation;
- the search for structural features, responsible for a compound's activity/inactivity (the features being fragments of molecular structures are referenced as pharmacophores/anti-pharmacophores, correspondingly).

To find pharmacophores, a template active compound and the rest of the compound set are compared as weighted graphs. To find anti-pharmacophores, an inactive compound is used as a template for the comparison. By this, molecular flexibility is taken into account when comparing atomic and bond weights for any two matrices. The essential part of the ETM is represented just by the last two steps.

The main advantages of the ETM are conditioned by the fact that its molecular descriptions reflect a molecule's electronic and 3D conformational properties and, at the same time, they do not depend on the numbers and sorts of atoms.

Table 1
Antituberculosis activities of compounds (**3**–**31**)

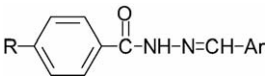

Compounds	R	Ar	Inhibition (%)	Compounds	R	Ar	Inhibition (%)
3	–F	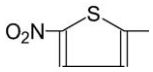	99	**18**	–F		17
4	–F	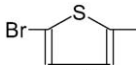	98	**19**	–F	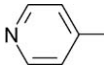	13
5	–NO2	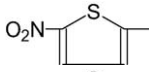	98	**20**	–F	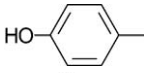	9
6	–Cl	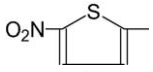	96	**21**	–H	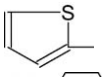	9
7	–H	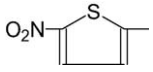	96	**22**	–F	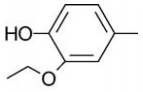	7
8	–F	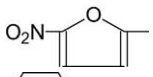	72	**23**	–F	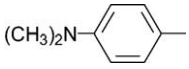	5
9	–F	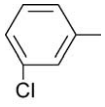	57	**24**	–F		5
10	–F	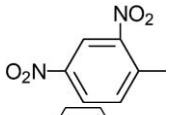	39	**25**	–F	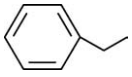	4
11	–F	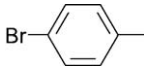	36	**26**	–F	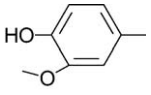	3
12	–F		35	**27**	–F	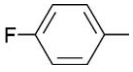	0
13	–Cl	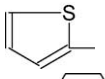	34	**28**	–F		0
14	–F	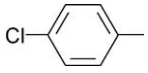	28	**29**	–F	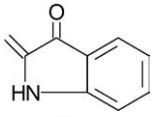	0
15	–F	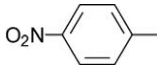	25	**30**	–Br		0
16	–F	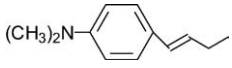	23	**31**	–NO_2		0
17	–F	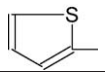	18				

MIC (μg/ml) < 6.25 for compounds **3**–**7**, and MIC > 6.25 for the rest of compounds.

Thus, for each compound (active or inactive) taken as a template, its ETMC was compared with the ETMCs of the rest of compounds in both classes of the series under study. The comparison resulted in a few common structural fragments for the two cases. The fragments were found as submatrices of template ETMCs (they will be referenced as Electron-Topological Submatrices of Contiguity, or ETSCs). Consequently, all pharmacophores and anti-pharmacophores found from the ETM calculations form a system for the activity identification [39–42].

For the series studied, the system includes 10 pharmacophores and 10 anti-pharmacophores. From compounds **3** and **5** chosen as active template compounds, activity features 1 and 2 (or the Ph1 and Ph2 pharmacophores) were found. They are shown in Fig. 1a,b by their corresponding ETSCs, which contain electronic-topological characteristics of these pharmacophores.

As seen from the Ph1 and Ph2 pharmacophore's structures, they consists of seven atoms for Ph1 (S_{13}, C_{14}, C_{15}, N_{16}, F_{19},

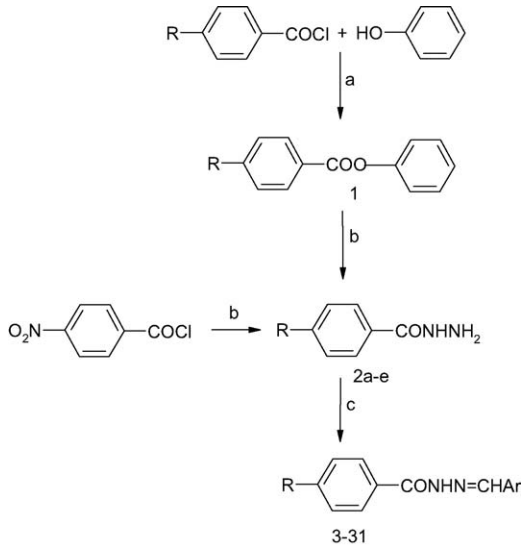

Scheme 1. Synthetic pathway for compounds **1**–**31**. R: H (a), Br (b), Cl (c), F (d), NO_2 (e).
Ar: Substituted phenyl/thiophenyl, furanyl, pyrolyl. Reagents and conditions: (a) NaOH; (b) NH_2NH_2 , CH_3OH; (c) RCHO, C_2H_5OH.

O_{20}, O_{21}) and seven atoms for Ph2 (C_7, C_{10}, C_{12}, C_{13}, C_{15}, C_{16}, O_{19}). Its submatrix is found after setting allowable limits for the search for equivalent matrix elements. The limits are δ_1 = ±0.05 (diagonal elements) and δ_2 = ±0.15 (off-diagonal ones). To evaluate the probability (P_A) of occurrence of a pharmacophore (Ph_i) in the series under study, one common criterion for structural methods is used as given by the following equation

$$P_A\ (Ph_i) = (n_1 + 1)/(n_1 + n_2 + 2) \quad (1)$$

where n_1, n_2 are numbers of active/inactive compounds, respectively, that contain the Ph. For an anti-pharmacophore (APh_i), ($n_2 + 1$) is to be used at place of ($n_1 + 1$) in Eq. (1). The pharmacophore found from the ETM-calculations is realized in five high-active compounds (**3**–**5**), and the probability P_A of its realization in this class is about 0.86. The remaining pharmacophores, Ph3–Ph10, have been found analogously, and the probabilities of their realization in the class of active compounds vary between 0.83 and 0.86.

To determine anti-pharmacophores ('break of activity'), ETMCs of inactive compounds were taken as templates. Ten anti-pharmacophores, APh1–APh10, were found in total. The ETSCs that correspond to APh1and APh2 are given in Fig. 2a, b along with structure of the corresponding template after which the anti-pharmacophores have been found.

As seen from Fig. 2a, APh1 (based on the inactive template **27**) consists of six atoms. APh1 is present in 22 inactive molecules, thus the probability of its realization is 0.96. Analysis of submatrices that correspond to APh1 and APh2 but are calculated relative to different template compounds, has shown their close similarity.

The highest occupied molecular orbitals (HOMO) and the lowest unoccupied molecular orbitals (LUMO), called also frontier orbitals, may well play an important role in the

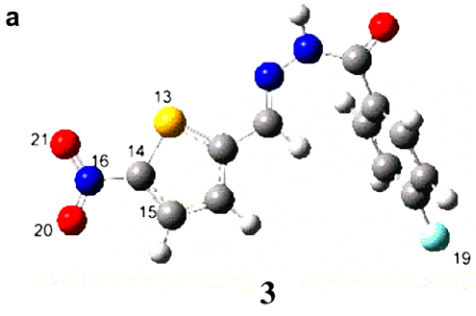

S_{13}	C_{14}	C_{15}	N_{16}	F_{19}	O_{20}	O_{21}
0.78	1.14	2.56	2.78	10.72	3.02	3.86
	-0.50	1.45	0.90	12.23	2.30	2.30
		-0.07	2.52	12.26	3.58	2.81
			0.61	13.50	1.44	1.46
				-0.10	13.57	14.52
					-0.37	2.10
						-0.35

$P_\alpha = 0.83$; n1/n2= 4/0

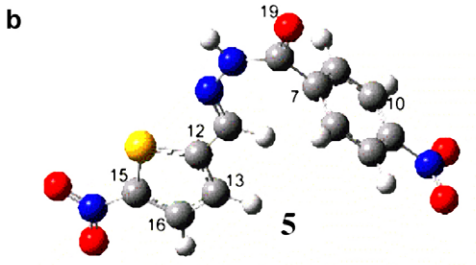

C_7	C_{10}	C_{12}	C_{13}	C_{15}	C_{16}	O_{19}
-0.12	2.81	6.53	7.62	8.75	8.82	3.54
	-0.07	8.14	9.05	10.49	10.36	4.31
		-0.35	1.45	2.43	2.32	4.26
			-0.15	2.32	1.36	4.91
				-0.50	1.45	6.69
					-0.07	6.29
						-0.33

$P_\alpha = 0.86$ n1/n2= 5/0

Fig. 1. Submatrices of the Ph1 and Ph2 pharmacophores (template compounds **3**(a), **5**(b)) and their corresponding structures.

donor-acceptor interaction of a substance with the corresponding receptors. Analysis of LUMOs for the compounds containing Ph1, and Ph2 has shown that atoms with the highest values of the atomic orbital coefficients are mainly those atoms that enter into the fragments. Graphical representation of LUMO orbitals is given in Fig. 3.

LUMO orbital for the template compound **3** (Fig. 3) consists of orbitals belonging to those atoms that form furanyl group and, partially, phenyl ring. Atoms representing Ph1 are mostly those that deposit considerably to the LUMO orbitals. Similar situation can be observed in the case of template compound **5**. In contrast to Ph1, LUMO orbital of APh1 consists of atoms of phenyl rings and hydrazide group. All the said suggests again an important role of these atoms in the substrate-receptor interaction.

Even inconsiderable changes in the molecular structure can affect the values of the corresponding ETMC and, in this way,

a

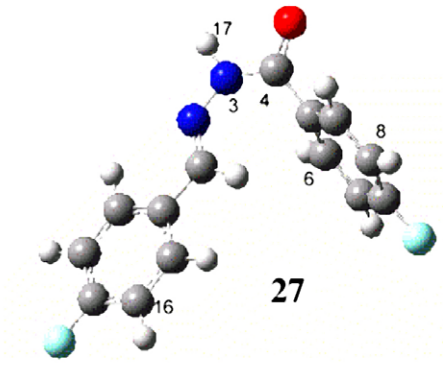

N_3	C_4	C_6	C_8	C_{16}	H_{17}
-0.30	1.03	3.00	4.77	6.06	0.88
	0.33	2.52	3.77	6.68	2.07
		-0.08	2.80	8.90	2.72
			-0.17	10.36	4.71
				-0.17	6.78
$P_\alpha = 0.96$; n1/n2= 0/22					0.26

b

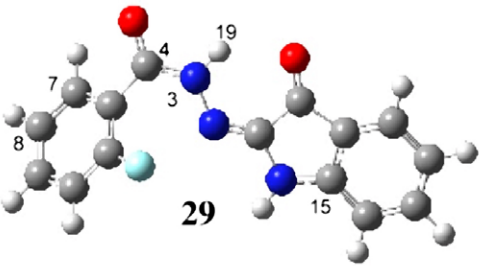

N_3	C_4	C_7	C_8	C_{15}	H_{19}
-0.30	0.98	3.58	4.77	5.97	0.86
	0.38	2.469	3.76	7.24	2.08
		-0.06	1.43	9.50	3.76
			-0.15	10.67	4.73
				-0.18	6.06
$P_\alpha = 0.96$; n1/n2= 0/22					0.25

Fig. 2. Submatrices of the APh1 and APh2 anti-pharmacophores (template compounds **27**(a), **29**(b)), and their corresponding structures.

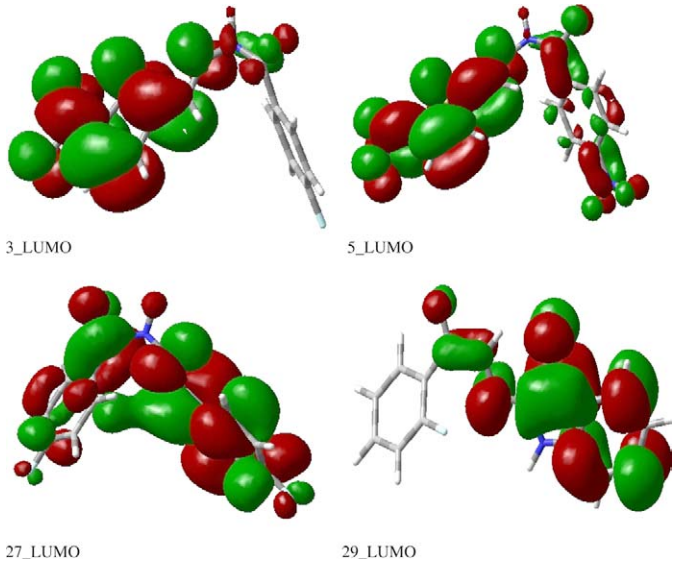

Fig. 3. A 3D-view of LUMO orbitals for template compounds **3**, **5**, **27** and **29**.

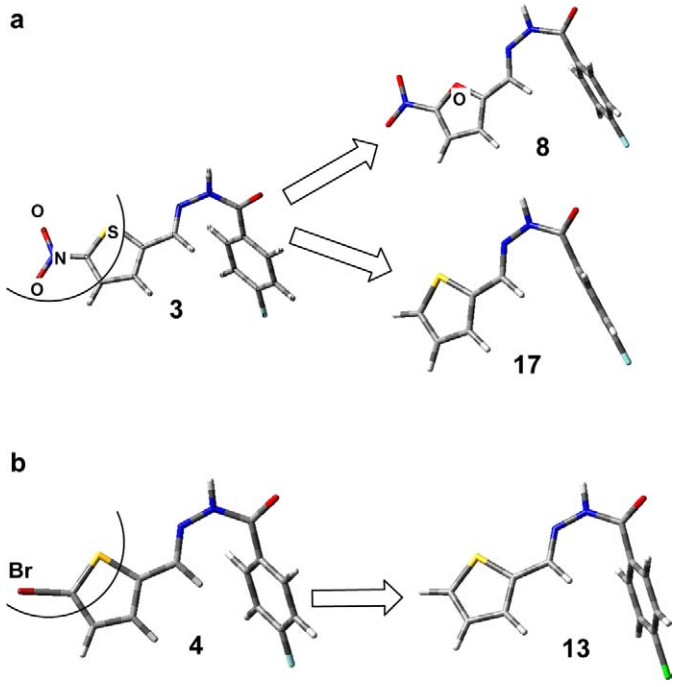

Fig. 4. Comparison of active and inactive molecules.

influence the compound's activity. For the template compound **3** some examples are given, which demonstrate the effects of its modifications on its activity (Fig. 4). As it was said above, the presence of thiophen ring and a voluminous electronegative group attached to it (NO_2, Br) is of great importance for the activity manifestation. Thus, when the atom of sulfur (compound **3**) is replaced by the oxygen atom, the thiophen ring transforms to furane ring, and activity of the resulting compound **8** is 27% lower, in comparison to the compound **3**. The absence of the NO_2 group in the thiophen ring deactivates compounds considerably (see compound **17**). Activity decreases by 81%. Analogous situation is observed when compound **4** transforms to compound **13**.

The sort of halogen in *para*-position to aromatic ring does not influence substantially the compound's activity (see compounds **3**, **5–7** in Table 2, Ph1).

Along with this, if NO_2-group in the thiophen ring is absent, activity decreases abruptly with the substituent replacement (compounds **13**, **17**, **21**, **30**). The thiophen ring replacement by phenyl, pyridine, and pyrole ring causes the decrease of activity as well (see compounds **4**, **11**, **15**, **19**, **28**).

When comparing the structures of the pharmacophores and anti-pharmacophores, one should pay close attention to the differences in their spatial and electronic characteristics.

Table 2
Substituents in *para*-position to aromatic ring and their influence on the compound's activity

1. R in phenyl, $-NO_2$ thiophene	–F (compound **3**)	$-NO_2$ (compound **5**)	–Cl (compound **6**)	–H (compound **7**)
MIC, %	99	98	96	96
2. R in phenyl,$-NO_2$ is absent	–F (compound **17**)	–Br (compound **30**), $-NO_2$ (compound **31**)	–Cl (compound **13**)	–H (compound **21**)
MIC, %	18	0	34	9

To test the system's capability of the antituberculosis activity prognostication, we modeled a few compounds with analogous structures. After their geometries had been optimized and their electronic structures had been calculated, ETMC matrices were formed. In concordance with the set of pharmacophores found, these compounds were classified by their activities as active ("+") and inactive ("−"). Structures of these compounds and their activities are presented in Table 3. For the compounds **T1**–**T6**, their predicted activities MIC > 70% (i.e. they are active compounds), while for the compounds **T7**–**T12** their expected MIC values are < 20% (inactive compounds).

Thus, the complex of pharmacophores and anti-pharmacophores taken as a whole plays an important role in the activities prediction as well as in the search for new drugs. The set of activity/inactivity fragments found as a result of this study forms a basis for the development of a system for the antituberculosis activity prediction.

4. Conclusions

A number of hydrazide–hydrazones were designed, synthesized, and screened for antituberculosis activity against *M. tuberculosis* H37Rv. A systematic SAR study of the compounds was performed through the application of the ETM relative to their experimentally measured antituberculosis activity. Data obtained from conformational analysis and quantum-chemistry calculations were used to form electronic-topological matrices. These matrices were effectively used in the search for a system of pharmacophores and anti-pharmacophores capable of effective separation of compounds from the examination set into groups of active and inactive compounds. Low-active molecules are badly responsive to the activity prognostication, because they form a buffer zone consisting of compounds that can include both pharmacophores and anti-pharmacophores. The model developed in this study is supposed to be applied to the design, preparation and screening of new compounds of similar structure in order to further test and optimize the model with the eventual goal of preparing new anti-tubercular agents.

5. Experimental

All chemicals and solvents were purchased from Merck, Aldrich, and Fluka. Melting points (m.p.) were determined with a Buchi 530 capillary apparatus and were uncorrected. ^{1}H-NMR spectra were recorded in DMSO on a Bruker AVANC-DPX-400 spectrometer in DMSO-d_6 and chemical shifts were given in δ ppm with tetramethylsilane (TMS). The splitting patterns of ^{1}H-NMR were designed as follows: s: singlet, d: doublet, t: triplet, q: quarlet, m. multiplet. The Mass spectrometry was performed using Agilent 1100 MSD spectrometer in the electrospray mode. All new compounds were analyzed for C, H, N and the results were in an acceptable range (^{1}H-NMR, mass and elemental analysis were provided by the Scientific and Technical Research Council of Turkey, TÜBITAK).

5.1. Antituberculosis activity

The primary screen is conducted at 6.25 μg/ml (or molar equivalent of highest molecular weight compound in a series of congeners) against *M. tuberculosis* H_{37}Rv (ATCC 27294) in BACTEC 12B medium using the MABA. Compounds exhibiting fluorescence are tested in the BACTEC 460-radiometric system. Compounds effecting < 90% inhibition in the primary screen (MIC > 6.25 μg/ml) are not generally evaluated further.

Table 3
Compounds of the examining set and their activities (predicted)

Compounds	R	Ar	Activity	Compounds	R	Ar	Activity
T1	$-OCH_3$	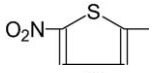	+	**T7**	$-OCH_3$		–
T2	$-CH_3$	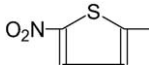	+	**T8**	$-CH_3$		–
T3	$-NH_2$	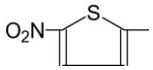	+	**T9**	$-NH_2$		–
T4	$-N(CH_3)_2$	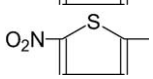	+	**T10**	$-N(CH_3)_2$		–
T5	–OH	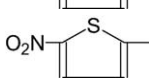	+	**T11**	–OH		–
T6	–CN	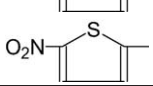	+	**T12**	–CN		–

Determination of MIC: Compounds demonstrating at least 90% inhibition in the primary screen are re-tested at lower concentrations against *M. tuberculosis* $H_{37}Rv$ to determine the actual MIC in the MABA. The MIC is defined as the lowest concentration effecting a reduction in fluorescence of 90% relative to controls.

5.2. Synthesis of 4-substituted phenyl benzoate (1)

To the solution of 0.1 mol of phenol in 100 ml of sodium hydroxide (10%), 0.1 mol of 4-fluorobenzoyl chloride was added and stirred for 30 min. The solid product was washed with distilled water and crystallized from ethanol [30].

5.3. Synthesis of 4-substituted benzoic acid hydrazide (2)

To the solution of 0.05 mol of **1** in 3 ml of methanol was added 0.1 mol of 99% hydrazine hydrate. The mixture was refluxed on a water bath for 30 min. After cooling, the precipitate was collected, washed with distilled water, and recrystallized from ethanol [18].

5.4. Synthesis of 4-substitutedbenzoic acid (substitutedmethylene) hydrazides (3–31)

A solution of 0.005 mol of substituted aldehydes in ethanol was added a solution of 0.005 mol of **2a**–**e** and isoniazide in 50 ml of ethanol. The mixture was refluxed on a water bath for 2–2.5 h. After cooling the mixture, the precipitate was filtered, dried and recrystallized from ethanol [11,18].

5.4.1. 4-Fluorobenzoic acid [((5-nitro)thiophen-2-yl) methylene]hydrazide (3)

Yield 87%, m.p. 275 °C. ^{1}H-NMR (DMSO-d_6, 400 MHz) δ (ppm) 7.39 (t, 2H, *ortho*-protons to F), 7.59 (d, 1H, *J*: 4.22 Hz, H_3 proton of thiophen), 7.95–8.05 (m, 2H, *meta*-protons to F), 8.15 (d, 1H, *J*: 4.33 Hz, H_4 proton of thiophen), 8.67 (s, 1H, =C–H), 12.25 (s, 1H, –NH). Anal. Calcd. for $C_{12}H_8FN_3O_3S$: C, 49.14; H, 2.73; N, 14.33; S, 10.92. Found: C, 48.97; H, 2.63; N, 14.15; S, 10.46. MS(ES): 294 (MH^+).

5.4.2. 4-Fluorobenzoic acid [(5-bromothiophen-2-yl) methylene]hydrazide (4)

Yield 93%, m.p. 190 °C. ^{1}H-NMR (DMSO-d_6, 400 MHz) δ (ppm) 7.19–7.89 (m, 6H, ArH), 8.49 (s, 1H, =C–H), 11.81 (s, 1H, –NH). Anal. Calcd. for $C_{12}H_8BrFN_2OS.H_2O$: C, 41.73; H, 2.89; N, 8.11; S, 9.27. Found: C, 41.65; H, 2.57; N, 8.06; S, 9.41. MS(ES): *m*/*z* 327 (MH^+), 329 (MH^+ + 2).

5.4.3. 4-Nitrobenzoic acid [((5-nitro)thiophen-2-yl)methylene] hydrazide (5)

Yield 84%, m.p. 240 °C. ^{1}H-NMR (DMSO-d_6, 400 MHz) δ (ppm) 7.64 (d, 1H, *J*: 4.27 Hz, H_3 proton of thiophen), 8.14–8.16 (m, 3H, H_4 proton of thiophen and *meta*-protons to NO_2), 8.40 (d, 2H, *J*: 8.66 Hz, *ortho*-protons to NO_2), 8.69 (s, 1H, =C–H), 12.51 (s, 1H, –NH). Anal. Calcd. for $C_{12}H_8N_4O_5S$: C, 45.00; H, 2.52; N, 17.49; S, 10.01. Found: C, 44.99; H, 2.40; N, 17.37; S, 9.58. MS(ES): *m*/*z* 321 (MH^+).

5.4.4. 4-Fluorobenzoic acid [(3-chlorophenyl)methylene]hydrazide (9)

Yield 80%, m.p. 165 °C. ^{1}H-NMR (DMSO-d_6, 400 MHz) δ (ppm) 7.38 (t, 2H, *ortho*-protons to F), 7.49 (d, 2H, *J*: 4.31 Hz, H_4 and H_6 protons), 7.70 (t, 1H, H_5 proton), 7.79 (s, 1H, H_2 proton), 7.99–8.02 (m, 2H, *meta*-protons to F), 8.43 (s, 1H, =C–H), 12.02 (s, 1H, –NH). Anal. Calcd. for $C_{14}H_{10}ClFN_2O$: C, 60.77; H, 3.64; N, 10.12. Found: C, 59.22; H, 4.18; N, 9.58. MS(ES): *m*/*z* 277 (MH^+), 279 (MH^+ + 2).

5.4.5. 4-Fluorobenzoic acid [(4-bromophenyl)methylene]hydrazide (11)

Yield 53%, m.p. 196 °C. ^{1}H-NMR (DMSO-d_6, 400 MHz) δ (ppm) 7.35–8.01 (m, 8H, ArH), 8.42 (s, 1H, =CH–), 11.93 (s, 1H, –NH). Anal. Calcd. for $C_{14}H_{10}BrFN_2O.H_2O$: C, 49.70; H, 3.55; N, 8.28. Found: C, 49.14; H, 3.40; N, 8.25. MS(ES): *m*/*z* 321 (MH^+), 323 (MH^+ + 2).

5.4.6. 4-Fluorobenzoic acid [(2-fluorophenyl)methylene]hydrazide (12)

Yield 80%, m.p. 215 °C. ^{1}H-NMR (DMSO-d_6, 400 MHz) δ (ppm) 7.95–8.04 (m, 8H, ArH), 8.60 (s, 1H, –CH=), 11.89(s, 1H, –NH). Anal. Calcd. for $C_{14}H_{10}F_2N_2O$: C, 64.61; H, 3.87; N, 10.76. Found: C, 63.92; H, 3.74; N, 10.65. MS(ES): *m*/*z* 261 (MH^+).

5.4.7. 4-Fluorobenzoic acid [(4-chlorophenyl)methylene]hydrazide (14)

Yield 75%, m.p. 182 °C. ^{1}H-NMR (DMSO-d_6, 400 MHz) δ (ppm) 7.38 (t, 2H, *ortho*-protons to F), 7.54 (d, 2H, *J*: 8.28 Hz, *ortho*-protons to Cl), 7.77 (d, 2H, *J*: 8.28 Hz, *meta*-protons to Cl), 7.98–8.02 (m, 2H, *meta*-protons to F), 8.45 (s, 1H, =C–H), 11.95 (s, 1H, –NH). Anal. Calcd. for $C_{14}H_{10}ClFN_2O$: C, 60.77; H, 3.64; N, 10.12. Found: C, 59.80; H, 3.60; N, 9.55. MS(ES): *m*/*z* 277 (MH^+), 279 (MH^+ + 2).

5.4.8. 4-Fluorobenzoic acid [(4-dimethylaminocinnamyl)methylene]hydrazide (16)

Yield 92%, m.p. 235–237 °C. ^{1}H-NMR (DMSO-d_6, 400 MHz) δ (ppm) 2.96 (s, 6H, $–CH_3$ protons of tert.amine), 6.72 (d, 2H, *J*: 8.75 Hz, *ortho*-protons to tert.amine), 6.76–6.82 (2d, 1H, =CH–C<u>H</u>=CH–), 6.92 (d, 1H, =CH–CH=C<u>H</u>–), 7.36 (t, 2H, *ortho*-protons to F), 7.45 (d, 1H, *J*: 8.75 Hz, *meta*-protons to tert.amine), 7.95–7.98 (m, 2H, *meta*-protons to F), 8.16 (d, 1H, *J*: 9.17 Hz, –CH=), 11.59 (s, 1H, –NH). Anal. Calcd. for $C_{18}H_{18}FN_3O$: C, 70.13; H, 6.20; N, 12.91. Found: C, 69.52; H, 5.76; N, 13.40. MS(ES): *m*/*z* 312 (MH^+).

5.4.9. 4-Fluorobenzoic acid [(thiophen-2-yl)methylene] hydrazide (17)

Yield 90%, m.p. 238 °C. ^{1}H-NMR (DMSO-d_6, 400 MHz) δ (ppm) 7.16 (t, 1H, H_4 proton of thiophen), 7.37 (t, 2H, *ortho*-protons to F), 7.49 (d, 1H, *J*: 3.13 Hz, H_3 proton of thiophen),

7.69 (d, 1H, *J*: 4.81 Hz, H_5 proton of thiophen), 7.96–8.00 (m, 2H, *meta*-protons to F) 8.66 (s, 1H, =C–H), 11.83 (s, 1H, –NH). Anal. Calcd. for $C_{12}H_9FN_2OS$: C, 58.05; H, 3.65; N, 11.28; S, 12.92. Found: C, 57.74; H, 3.46; N, 11.30; S, 12.78. MS(ES): *m*/*z* 249 (MH^+).

*5.4.10. 4-Fluorobenzoic acid [(2-hydroxyphenyl)methylene]hydrazide (**18**)*

Yield 82%, m.p. 190 °C. ^{1}H-NMR (DMSO-d_6, 400 MHz) δ (ppm) 6.96 (t, 2H, *ortho*-protons to F), 7.29–7.33 (m, 1H, H_5 proton), 7.39 (t, 2H, H_4 and H_6 protons), 7.56 (d, 1H, *J*: 8.77 Hz, H_3 proton), 8.01–8.04 (m, 2H, *meta*-protons to F), 8.65 (s, 1H, =C–H), 11.25 (s, 1H, –OH), 12.13 (s, 1H, –NH). Anal. Calcd. for $C_{14}H_{11}FN_2O_2$: C, 65.11; H, 4.29; N, 10.85. Found: C, 64.36; H, 4.15; N, 10.28. MS(ES): *m*/*z* 259 (MH^+).

*5.4.11. 4-Fluorobenzoic acid [(pyridyl-4-yl)methylene] hydrazide (**19**)*

Yield 80%, m.p. 224 °C. ^{1}H-NMR (DMSO-d_6, 400 MHz) δ (ppm) 7.28–8.58 (m, 8H, ArH), 8.35 (s, 1H, =C–H), 12.05 (s, 1H, –NH). Anal. Calcd. for $C_{13}H_{10}FN_3O$: C, 64.19; H, 4.14; N, 17.28. Found: C, 63.34; H, 4.86; N, 17.21. MS(ES): *m*/*z* 244 (MH^+).

*5.4.12. 4-Fluorobenzoic acid [(4-hydroxyphenyl)methylene]hydrazide (**20**)*

Yield 65%, m.p. 260 °C. ^{1}H-NMR (DMSO-d_6, 400 MHz) δ (ppm) 6.85 (d, 2H, *J*: 8.44 Hz, *ortho*-protons to OH), 7.36 (t, 2H, *ortho*-protons to F), 7.57 (d, 2H, *J*: 8.44 Hz, *meta*-protons to OH), 7.96–8.00 (m, 2H, *meta*-protons to F), 8.34 (s, 1H, –CH=), 9.94 (s, 1H, –OH), 11.67 (s, 1H, –NH). Anal. Calcd. for $C_{14}H_{11}FN_2O_2$: C, 65.11; H, 4.29; N, 10.85. Found: C, 65.29; H, 4.52; N, 10.95. MS(ES): *m*/*z* 259 (MH^+).

*5.4.13. 4-Fluorobenzoic acid [(4-hydroxy-3-ethoxyphenyl) methylene]hydrazide (**22**)*

Yield 66%, m.p. 215 °C. ^{1}H-NMR (DMSO-d_6, 400 MHz) δ (ppm) 1.37 (t, 3H, $-CH_2\underline{CH_3}$), 4.08 (q, 2H, $-\underline{CH_2}CH_3$), 6.87 (t, 1H, H_5 proton), 7.09 (d, 1H, *J*: 8.12 Hz, H_6 proton), 7.30 (s, 1H, H_2 proton), 7.36 (t, 2H, *ortho*-protons to F), 7.96–8.00 (m, 2H, *meta*-protons to F), 8.32 (s, 1H, =CH–), 9.50 (s, 1H, –OH), 11.68 (s, 1H, –NH). Anal. Calcd. for $C_{16}H_{15}FN_2O_3$: C, 63.57; H, 5.00; N, 9.27. Found: C, 63.93; H, 4.85; N, 9.29. MS (ES): *m*/*z* 303 (MH^+).

*5.4.14. 4-Fluorobenzoic acid [(4-dimethylaminophenyl)methylene]hydrazide (**23**)*

Yield 80%, m.p. 183–184 °C. ^{1}H-NMR (DMSO-d_6, 400 MHz) δ (ppm) 2.98 (s, 6H, CH_3 protons of tert.amine), 6.76 (d, 2H, *J*: 8.85 Hz, *ortho*-protons to tert.amine), 7.35 (t, 2H, *ortho*-protons to F), 7.55 (d, 2H, *J*: 8.85 Hz, *meta*-protons to tert.amine), 7.96–7.99 (m, 2H, *meta*-protons to F), 8.31 (s, 1H, –CH=), 11.57 (s, 1H, –NH). Anal. Calcd. for $C_{16}H_{16}FN_3O$: C, 67.35; H, 5.65; N, 14.73. Found: C, 66.86; H, 5.08; N, 14.03. MS(ES): *m*/*z* 286 (MH^+).

*5.4.15. 4-Fluorobenzoic acid [(2-furanyl)methylene]hydrazide (**24**)*

Yield 82%, m.p. 193–194 °C. ^{1}H-NMR (DMSO-d_6, 400 MHz) δ (ppm) 6.56 (s, 1H, H_4 proton of furan), 6.86 (d, 1H, *J*: 3.10 Hz, H_3 proton of furan), 7.28 (t, 2H, *ortho*-protons to F), 7.77 (s, 1H, H_5 proton of furan), 7.87–7.90 (m, 2H, *meta*-protons to F), 8.24 (s, 1H, –CH=), 11.72 (s, 1H, –NH). Anal. Calcd. for $C_{12}H_9FN_2O_2$: C, 62.07; H, 3.91; N, 12.06. Found: C, 61.61; H, 3.58; N, 12.09. MS(ES): *m*/*z* 233 (MH^+).

*5.4.16. 4-Fluorobenzoic acid [(benzyl)methylene]hydrazide (**25**)*

Yield 40%, m.p. 153 °C. ^{1}H-NMR (DMSO-d_6, 400 MHz) δ (ppm) 4.49 (s, 2H, $–CH_2–$), 7.28–7.88 (m, 9H, aromatic protons), 8.30 (s, 1H, =CH–), 11.90 (s, 1H, –NH). Anal. Calcd. for $C_{15}H_{13}FN_2O$: C, 70.30; H, 5.11; N, 10.93. Found: C, 69.29; H, 5.14; N, 10.78. MS(ES): *m*/*z* 257 (MH^+).

*5.4.17. 4-Fluorobenzoic acid [(4-hydroxy-3-methoxyphenyl) methylene]hydrazide (**26**)*

Yield 82%, m.p. 183 °C. ^{1}H-NMR (DMSO-d_6, 400 MHz) δ (ppm) 3.84 (s, 3H, CH_3 protons), 6.85 (d, 1H, *J*: 8.11 Hz, H_5 proton), 7.09 (d, 1H, *J*: 8.09 Hz, H_6 proton), 7.32–7.39 (m, 3H, H_2 proton and *ortho*-protons to F), 7.96–8.00 (m, 2H, *meta*-protons to F), 8.34 (s, 1H, –CH=), 9.57 (s, 1H, –OH), 11.48 (s, 1H, –NH). Anal. Calcd. for $C_{15}H_{13}FN_2O_3$: C, 62.50; H, 4.55; N, 9.72. Found: C, 62.25 H; 4.03; N, 9.76. MS(ES): *m*/*z* 289 (MH^+).

*5.4.18. 4-Fluorobenzoic acid [(4-fluorophenyl)methylene]hydrazide (**27**)*

Yield 90%, m.p. 184–185 °C. ^{1}H-NMR (DMSO-d_6, 400 MHz) δ (ppm) 7.31 (t, 2H, *meta*-protons to –CONH), 7.37 (t, 2H, *meta*-protons to –N=CH), 7.78–7.82 (m, 2H, *ortho*-protons to –CONH), 7.98–8.02 (m, 2H, *ortho*-protons to –N=CH), 8.45 (s, 1H, –CH=), 11.89 (s, 1H, –NH). Anal. Calcd. for $C_{14}H_{10}F_2N_2O$: C, 64.61; H, 3.87; N, 10.76. Found: C, 64.75; H, 4.04; N, 10.15. MS(ES): *m*/*z* 261 (MH^+).

*5.4.19. 4-Fluorobenzoic acid [(pyrole-2-yl)methylene] hydrazide (**28**)*

Yield 92%, m.p. 217 °C. ^{1}H-NMR (DMSO-d_6, 400 MHz) δ (ppm) 6.06 (s, 1H, H_4 proton of pyrole), 6.40 (s, 1H, H_3 proton of pyrole), 6.83 (s, 1H, H_5 proton of pyrole), 7.26 (t, 2H, *ortho*-protons to F), 7.86–7.90 (m, 2H, *meta*-protons to F), 8.18 (s, 1H, =C–H), 11.45 (s, 2H, –NH of hydrazone and –NH of pyrole). Anal. Calcd. for $C_{12}H_{10}FN_3O.H_2O$: C, 57.83; H, 4.81; N, 16.87. Found: C, 57.78; H, 4.82; N, 16.96. MS (ES): *m*/*z* 232 (MH^+).

*5.4.20. 2-[(Fluorobenzoyl)hydrazono]-1,3-dihydro-indol-3-one (**29**)*

Yield 95%, m.p. 283 °C. ^{1}H-NMR (DMSO-d_6, 400 MHz) δ (ppm) 6.87 (d, 1H, *J*: 7.83 Hz, H_7 proton of indole), 7.03 (t, 1H, H_6 proton of indole), 7.30–7.39 (m, 3H, *ortho*-protons to F

and H_5 proton of indole), 7.52 (d, 1H, *J*: 7.44 Hz, C_4 proton of indole), 7.86–7.90 (m, 2H, *meta*-protons to F), 11.15 (s, 1H, –NH), 13.89 (s, 1H, –NH of indole). Anal. Calcd. for $C_{15}H_{10}FN_3O_2$: C, 63.60; H, 3.56; N, 14.83. Found: C, 63.58; H, 3.76; N, 14.91. MS(ES): *m*/*z* 284 (MH^+).

5.5. Antituberculosis activity

The primary screen is conducted at 6.25 μg/ml (or molar equivalent of highest molecular weight compound in a series of congeners) against *M. tuberculosis* $H_{37}Rv$ (ATCC 27294) in BACTEC 12B medium using the MABA. Compounds exhibiting fluorescence are tested in the BACTEC 460-radiometric system. Compounds effecting < 90% inhibition in the primary screen (MIC > 6.25 μg/ml) are not generally evaluated further.

Determination of MIC: Compounds demonstrating at least 90% inhibition in the primary screen are re-tested at lower concentrations against *M. tuberculosis* $H_{37}Rv$ to determine the actual MIC in the MABA. The MIC is defined as the lowest concentration effecting a reduction in fluorescence of 90% relative to controls.

Determination of 50% inhibitory concentrations (IC_{50}): Concurrent with the determination of MICs, compounds are tested for cytotoxicity (IC_{50}) in vero cells at concentrations less than or equal to 62.5 μg/ml or 10 times the mıc for *m. tuberculosis* $H_{37}Rv$. after 72 hours exposure, viability is assessed on the basis of cellular conversion of mtt into a formazan product using the promega celltiter 96 non-radioactive cell proliferation assay.

Acknowledgements

This research was supported by The Research Fund of Marmara University, project number SAG-BGS-270605-0138. We thank Dr. Joseph A. Maddry from Tuberculosis Antimicrobial Acquisition and Coordinating Facility (TAACF) Southern Research Institute for his assistance.

References

[1] World Health Organization, in Anti-tuberculosis drug resistance in the world. The WHO/IUATLD global project on anti-tuberculosis drug resistance surveillance, 1997.
[2] C. Loncle, J.M. Brunel, N. Vidal, M. Dherbomez, Y. Letourneux, Eur. J. Med. Chem. 39 (2004) 1067–1071.
[3] S. Papakonstantinou-Garoufalias, N. Pouli, P. Marakos, A. Chytyroglou-Ladas, Farmaco 57 (2002) 973–977.
[4] P. Vicini, F. Zani, P. Cozzini, I. Doytchinova, Eur. J. Med. Chem. 37 (2002) 553–564.
[5] F.D. Popp, Eur. J. Med. Chem. 24 (1989) 313–315.
[6] S.K. Sridhar, S.N. Pandeya, J.P. Stables, R. Atmakuru, Eur. J. Pharm. Sci. 16 (2002) 129–132.
[7] S.G. Küçükgüzel, A. Mazi, F. Sahin, S. Öztürk, J.P. Stables, Eur. J. Med. Chem. 38 (2003) 1005–1013.
[8] A.R. Todeschini, A.L.P. Miranda, K.C.M. Silva, S.C. Parrini, E.J. Barreiro, Eur. J. Med. Chem. 33 (1998) 189–199.
[9] M.A. Gaston, L.R.S. Dias, A.C.C. Freitas, A.L.P. Miranda, E.J. Barreiro, Pharmac, Acta Helvet. 71 (1996) 213–219.
[10] P. Melnyk, V. Leroux, C. Sergheraert, P. Grellier, Bioorg. Med. Chem. Lett. 16 (2006) 31–35.
[11] Ş.G. Küçükgüzel, S. Rollas, I. Küçükgüzel, M. Kiraz, Eur. J. Med. Chem. 34 (1999) 1093–1100.
[12] B.K. Kaymakçıoğlu, S. Rollas, Farmaco 57 (2002) 595–599.
[13] J. Patole, U. Sandbhor, S. Padhye, D.N. Deobagkar, C.E. Anson, A. Powell, Bioorg. Med. Chem. Lett. 13 (2003) 51–55.
[14] R. Maccari, R. Ottanà, M.G. Vigorita, Bioorg. Med. Chem. Lett. 15 (2005) 2509–2513.
[15] M.T. Cocco, C. Congiu, V. Onnis, M.C. Pusceddu, M.L. Schivo, A. Logu, Eur. J. Med. Chem. 34 (1999) 1071–1076.
[16] N. Karalı, A. Kocabalkanlı, A. Gürsoy, Ö. Ateş, Farmaco 57 (2002) 589–593.
[17] D.G. Rando, D.N. Sato, L. Siqueira, A. Malvezzi, C.Q.F. Leite, A.T. Amaral, E.I. Ferreira, L.C. Tavares, Bioorg. Med. Chem. 10 (2002) 557–560.
[18] S. Rollas, N. Gulerman, H. Erdeniz, Farmaco 57 (2002) 171–174.
[19] A. Dimoglo, E. Sim, N. Shvets, V. Ahsen, Mini Rev. Med. Chem. 3 (2003) 293–306.
[20] A.S. Dimoglo, N.M. Shvets, I.V. Tetko, D.J. Livingstone, Quant. Struct.-, Act. Relat. 20 (2001) 31–45.
[21] A.S. Dimoglo, Khim.- pharm., Zhur. 4 (1985) 438–444.
[22] I.B. Bersuker, A.S. Dimoglo, Reviews in Computational Chemistry, in: K.B. Lipkowitz, D.B. Boyd (Eds.), VCH, New-York, 1991, pp. 423–460.
[23] N.M. Shvets, A.S. Dimoglo, Nahrung 42 (1998) 364–370.
[24] A.S. Dimoglo, A.A. Beda, N.M. Shvets, M.Y. Gorbachov, L.A. Kheifits, I.S. Aulchenko, N. J. Chem. 19 (1995) 149–155.
[25] A.S. Dimoglo, P.F. Vlad, N.M. Shvets, M.N. Coltsa, J. New, Chem. 25 (2001) 283–288.
[26] N.M. Shvets, A.S. Dimoglo, (ETM): its further development and use in the problems of SAR study, in: "Molecular Modeling and Prediction of Bioactivity" K. Gundertofte, F.S. Jorgensen (Eds.), Kluwer Academic/Plenum Publishers, The Electronic-Topological Method, New York, 1999, pp. 418–429.
[27] F. Kandemirli, N. Tokay, N. Shvets, A. Dimoglo, Arzneim. Forsh.- Drug Res 53 (2003) 133–138 (II).
[28] N. Shvets, A. Terletskaya, A. Dimoglo, Y.J. Chumakov, Mol. Sruct. Teochem. 463 (1999) 105–110.
[29] F. Macaev, G. Rusu, S. Pogrebnoi, A. Gudima, E. Stingaci, L. Vlad, N. Shvets, F. Kandemirli, A. Dimoglo, R. Reynolds, Bioorg. Med. Chem. 13 (2005) 4842–4850.
[30] E.E. Oruc, S. Rollas, F. Kandemirli, N. Shvets, A. Dimoglo, J. Med. Chem. 47 (2004) 6760–6767.
[31] A. Tossidis-Ioannis, Chem. Chron. 1983, 12(4), 181–197, Chemical Abstract 102 (1985) 6129v.
[32] A. Masunari, F.L. Lopes do Nascimento, M. Furlanetto, M.G. Baptista dos Santos, T.C.V. Penna, E.M. Mamizuka, L.C. Tavares, Revista Brasileira de Ciencias Farmaceuticas, 2003, 39 (Supl.3), 192–194, Chemical Abstract 141 (2004) 153674.
[33] F. Fujikawa, K. Hirai, O. Sawada, H. Toyoshima, S. Tamura, M. Naito, S. Tsukuma, Yakugaku Zasshi, 1962, 82, 1681–1684, Chemical Abstract 59 (1963) 2764g.
[34] T.A.A.C.F. Web Site, http://www.taacf.org.
[35] M.J. Frisch, G.W. Trucks, H.B. Schlegel, et al., Gaussian 98, Revision A.9, Gaussian, Inc, Pittsburgh, PA, 1998.
[36] N.M. Shvets, Comp. Sci. J. of Moldova 1 (3) (1993) 101–110.
[37] N.M. Shvets, Comp. Sci. J. of Moldova 5 (3) (1997) 301–311.
[38] N.M. Shvets, A. Terletskaya, A.S. Dimoglo, Y.M. Chumakov, Teochem. 463 (1999) 105–110 (J. Mol. Str.).
[39] F. Kandemirli, Arzneim.-Forsch. Drug Res. 52–10 (2002) 731–739.
[40] F. Kandemirli, M. Saraçoğlu, V. Kovalishyn, Mini Rev. Med. Chem. 5 (2005) 479–487.
[41] F. Kandemirli, N. Shvets, V. Kovalishyn, A. Dimoglo, J. Molec. Graph. Modell. (2006) (doi : 10.1016/i.jmgm.2005.10.011).
[42] F. Kandemirli, N. Shvets, S. Ünsalan, I. Küçükgüzel, S. Rollas, V. Kovalishyn, A. Dimoglo, Med. Chem. 2 (2006) 415–422.